Electronic Structure of Two-Dimensional Hydrocarbon Networks of sp2 and sp3 C Atoms

Electronic Structure of Two-dimensional Hydrocarbon Networks of sp^2 and sp^3 C Atoms

Yasumaru Fujii[1], Mina Maruyama[1], Katsunori Wakabayashi[2], Kyoko Nakada[3], and Susumu Okada[1*]

[1]*Graduate School of Pure and Applied Science, University of Tsukuba, 1-1-1 Tennodai, Tsukuba 305-8571, Japan*

[2]*Department of Nanotechnology for Sustainable Energy, School of Science and Technology, Kwansei Gakuin University, Gakuen 2-1, Sanda 669-1337, Japan*

[3]*Department of Chemistry and Biological Science, Aoyama Gakuin University, 5-10-1 Fuchinobe, Chuo-ku, Sagamihara 252-5258, Japan*

Based on density functional theory with the generalized gradient approximation, we have investigated the geometric and electronic structures of two-dimensional hexagonal covalent networks consisting of oligoacenes and fourfold coordinated hydrocarbon atoms, which are alternately arranged in a hexagonal manner. All networks were semiconductors with a finite energy gap at the Γ point, which monotonically decreased with the increase of the oligoacene length. As a result of a Kagome network of oligoacene connected through sp^3 C atoms, the networks possess peculiar electron states in their valence and conduction bands, which consist of a flat dispersion band and a Dirac cone. The total energy of the networks depends on the oligoacene length and has a minimum for the network comprising naphthalene.

1. Introduction

The electronic structure of nanoscale materials comprising sp^2 C atoms is characterized by their size, shape, and local atomic structures. Polycyclic aromatic hydrocarbon (PAH) molecules are representative examples that exhibit interesting variations in their electronic structure [1]. Oligoacene molecules basically possess a symmetric electronic structure with respect to the Fermi level and a moderate energy gap between the highest occupied and the lowest unoccupied states. This gap is inversely proportional to the size of oligoacene [1]. Besides the closed-shell electronic structure, PAHs with a triangular shape, such as phenalenyl and triangulene, possess radical spin states as their ground states in which the spin state depends on the sublattice imbalance in these triangular PAHs [2,3,4]. In addition to the PAHs, covalent networks consisting of these PAHs possess a unique electronic structure arising from the electronic structure of the constituent PAHs and boundary conditions imposed on the networks [5-12]. Graphene nanoribbons with zigzag edges have a pair of flat dispersion bands around the Brillouin zone boundary because of the delicate balance of the electron transfer around the edge atomic sites [7-10]. Dirac cones and Kagome flat bands coexist at/near the Fermi level in two-dimensional covalent hydrocarbon networks in which the hexagonally arranged phenalenyls are connected by a phenyl or oligoacene [11,12].

In addition to the planar hydrocarbon molecules, hydrocarbon molecules possessing three-dimensional covalent networks are considered by introducing the sp^3 C atoms in addition to sp^2 C atoms. Propellene [13-16] and triptycene [17-21] are representative examples of such three-dimensional aromatic hydrocarbon molecules with D_{3h} symmetry and Y-shaped ridged covalent frameworks consisting of three planar sp^2 networks connected by bridgehead sp^3 C atoms situated at the molecular axis. The ridged Y-shape networks of triptycene and propellene allow them to have a constituent unit for covalent organic frameworks: oligomerization and polymerization of triptycene and propellene result in porous and covalent architectures [22-26], which are expected to exhibit unusual electronic properties. In our previous work, two-dimensional covalent networks consisting of [4,4,4]propellene and sp^2 hydrocarbons possess a flat dispersion band at and around the Fermi level because the sp^2 hydrocarbon units form a Kagome lattice in the covalent network [26]. In addition, although triptycene can also form such two-dimensional networks, their energetics and electronic structures are still unclear. In particular, it is unclear how the energetics and electronic structures depend on the oligoacene species bridging the sp^3 C atoms.

In this work, we aim to investigate the energetics and electronic structures of

two-dimensional covalent networks comprising sp^3 hydrocarbons and oligoacenes, in terms of the size of oligoacene, using the density functional theory (DFT) with the generalized gradient approximation (GGA). Our calculations showed that all covalent networks are semiconductors irrespective of the oligoacene species, where the band gap monotonically decreases with increasing the oligoacene length. The covalent networks possess Kagome bands, which consist of a flat dispersion band throughout the Brillouin zone and two dispersive states forming a Dirac cone at the K point, in their valence and conduction bands, owing to the Kagome topology of oligoacene in the covalent networks. The network consisting of naphthalene and a sp^3 C bridgehead is the most energetically stable network among the networks consisting of oligoacenes ranging from benzene to pentacene.

2. Calculation Method and Structural Models

All calculations were based on DFT [27,28] as implemented in the program package Simulation Tools for Atom Technology (STATE) [29]. We used GGA with the Perdew–Burke–Ernzerhof functional to describe the exchange-correlation potential among interacting electrons [30]. Ultrasoft pseudopotentials generated by the Vanderbilt scheme were adopted as the interaction between electrons and ions [31]. Valence wave functions and the deficit charge density were expanded in terms of plane-wave basis sets with cutoff energies of 25 and 225 Ry, respectively, which give sufficient convergence in the total energy and electronic structures of covalent networks consisting of both sp^2 and sp^3 C atoms [32,33].   Molecular dynamics simulations were conducted using the velocity scaling method to keep the temperature constant during the simulation. Integrations over the Brillouin zones of the two-dimensional covalent network were executed by using equidistant 4×4×1 or 2×2×1 k-meshes, depending on the length of the oligoacene: the 4×4×1 k-mesh was adopted to the networks consisting of benzene and the 2×2×1 k-mesh was adopted to the networks consisting of naphthalene or longer oligoacenes. Lattice parameters and internal atomic structures were fully optimized until the force acting on each atom was less than 5 mRy/Å. To simulate an isolated two-dimensional hydrocarbon network, the two-dimensional covalent network was separated from its periodic images by a 10 Å vacuum spacing.

In this work, we consider two-dimensional covalent networks consisting of oligoacene (benzene, naphthalene, anthracene, tetracene, and pentacene) which are connected by sp^3 C atoms, resulting in a honeycomb network of sp^2 and sp^3 C atoms (Fig. 1). As far as the π electron states are concerned, the networks could be regarded as Kagome networks of oligoacene on which the π electron is transferred to its adjacent oligoacene through next nearest neighbor hopping because each oligoacene is separated by bridgehead sp^3 C atoms.

3. Results and Discussion

The optimized bond lengths of the two-dimensional covalent networks of sp^2 and sp^3 hydrocarbons are summarized in Table 1 under the equilibrium lattice constants of 8.92, 13.17, 17.44, 21.56, and 25.82 Å for the networks consisting of benzene, naphthalene, anthracene, tetracene, and pentacene, respectively. The bond length strongly depended on the mutual arrangement in the networks and oligoacene species owing to the bond alternation induced by the long bond associated with the sp^3 C atoms. The bonds associated with a zigzag chain of oligoacene clearly exhibited a bond alternation induced by the long covalent bond adjoining oligoacene and an sp^3 C atom. The bond alternation depended on the oligoacene length: the bond alternation in the network with long oligoacene was more significant than that with the short oligoacene. However, the bonds connecting two zigzag edges of oligoacene, d_1, d_4, and d_7, were monotonically elongated with the increase of oligoacene length. Furthermore, with an increase in the separation from the bridgehead sp^3 C atoms, the length of the perpendicular bonds also increased monotonically. The dynamical stability of the two-dimensional covalent networks of sp^2 and sp^3 hydrocarbons was investigated by *ab initio* molecular dynamics simulations conducted at a constant temperature of 1000 K for simulation times of 1 ps for the networks consisting of benzene, naphthalene, anthracene, and tetracen, and for simulation times of 0.2 ps for the network consisting of pentacene. Under the temperature, all structures retained their initial covalent network topologies after the simulation times of 1 and 0.2ps. Thus, we confirm that the two-dimensional covalent networks of sp^2 and sp^3 hydrocarbons proposed here are both statically and dynamically stable under ambient conditions once they are synthesized experimentally.

Figure 2 shows the total energy per C atom of two-dimensional covalent networks as a function of the oligoacene length. The total energy anomalously depended on the oligoacene length: the total energy exhibited a minimum for the network comprising naphthalene, even though the benzene molecule was the most stable among the oligoacene molecules studied here. However, the kinetic energy of the itinerant π electrons extending throughout the networks decreased with the increase in the size of the network. Therefore, an anomalous energy in terms of the oligoacene length was ascribed to the interplay between the itineracy and aromaticity of the π electron on the covalent network of sp^2 and sp^3 C atoms.

Figure 3 shows the electronic structure of two-dimensional covalent networks. All networks were semiconductors with the finite energy gap at the Γ point and a peculiar electronic structure in both their valence and conduction states. Most of the electron states

4

consisted of three branches, two of which had substantial dispersion forming a Dirac cone at the K point while the remaining state exhibited a flat band nature throughout the Brillouin zone. The characteristic dispersion relation of the three branches indicated that the electronic structures around the gap of these materials could be classified as a Kagome band structure, even though they were not the simple Kagome lattice. These Kagome bands strongly depended on the oligoacene length, although all networks possessed the same topology. The eigenvalues of these Kagome bands depended on the oligoacene length. The Kagome bands of the valence band top and that of the conduction band bottom gradually shifted upward and downward, respectively, with the increase of the oligoacene length. These facts imply that the oligoacene caused these peculiar Kagome bands of the two-dimensional covalent networks. The Kagome flat bands around the band gap provide the two-dimensional covalent networks constituent materials for optical devices with remarkable absorption efficiency caused by the interband transition between the flat band states. Furthermore, the networks may exhibit unusual magnetic ordering throughout the sp^2 C atoms by injecting the appropriate number of electron and hole into the conduction and valence Kagome flat bands, respectively.

To investigate the physical origin of the Kagome bands, we analyzed the wave function of the Kagome bands at the Γ point (Fig. 4). The distribution of the Kagome bands can be interpreted as the electron states of an isolated oligoacene. Each Kagome band split into upper and lower branches at the Γ point: the wave function of the lower Kagome states overlapped with those belonging to the adjacent oligoacene with the bonding nature. In contrast, the upper Kagome state exhibited an antibonding nature with its adjacent oligoacene states. The characteristics distribution of the wave function corroborates that the Kagome bands were ascribed to the electron hopping among the electron states of oligoacene which formed a Kagome network with the sp^3 C vertices. Therefore, the two-dimensional covalent frameworks could be regarded as the Kagome lattice with an internal degree of freedom.

The monotonic decrease of the band gap also reflected the fact that the Kagome band was ascribed to the highest occupied and the lowest unoccupied states of oligoacene arranged in a Kagome network. Figure 5 shows the band gap of the two-dimensional covalent networks as a function of the oligoacene length. The band gap monotonically decreased with increasing the oligoacene length except for the network comprising a benzene ring. Furthermore, the gap value of the network approximately corresponded to the energy gap between the lowest unoccupied and the highest occupied states of the constituent oligoacene molecule. Note that the narrow band gap of the network with benzene was ascribed to the unusual wave function distribution of the highest occupied state. Orbital hybridization between adjacent benzene rings prevented the usual distribution of the highest occupied

states of an isolated benzene molecule.

Figure 6 shows the bandwidth of Kagome bands as a function of the oligoacene length. Although the π electron was extended throughout the oligoacene in the two-dimensional covalent network, the bandwidth of the Kagome bands, K1, K2, and K3, monotonically decreased with increasing the oligoacene length for most cases. The monotonic decrease of the bandwidth originated from the nodal distribution of these states with respect to the network. However, the Kagome band K4 exhibited an opposite feature to the other Kagome bands: the bandwidth monotonically increased with increasing the oligoacene length. In this case, the wave functions associated with the state were distributed along the zigzag chains of oligoacene with bonding nature. Thus, the states were sensitive to hybridization with the wave functions of the adjacent oligoacene, leading to the increase of the bandwidth.

4. Conclusions

Using DFT with GGA, we studied the energetics and electronic structure of a hexagonal covalent organic framework consisting of oligoacene and bridgehead sp^3 hydrocarbons. All covalent networks were semiconductors where the band gap monotonically decreased with increasing the oligoacene length. The networks possess Kagome bands, which consist of a flat band throughout the Brillouin zone and two dispersive states forming a Dirac cone at the K point, in their valence and conduction bands, because oligoacenes form a Kagome network where they are connected through sp^3 hydrocarbon. The wave function analysis unraveled the physical origin of the Kagome band of the networks: the wave functions of the π electron states of the oligoacene are substantially hybridized with those of its three adjacent oligoacene. We also demonstrated that the network consists of naphthalene and bridgehead sp^3 C atoms is the most energetically stable among the networks consisting of oligoacene ranging from benzene to pentacene, owing to the interplay between the itineracy and aromaticity of π electrons distributed throughout the networks.

University and on an SGI ICE XA/UV at the Institute of Solid State Physics, The University of Tokyo.

*sokada@comas.frsc.tsukuba.ac.jp

References

1). E. Clar, The Aromatic Sextet (John Wiley and Sons, London, U.K. 1972).

2). Y. Morita, S. Suzuki, K. Sato, and T. Takui, Nature Chem. **3**, 197 (2011).

3). V. Boekelheide and C. E. Larrabee, J. Am. Chem. Soc. **72**, 1245 (1950).

4). D. H. Reid, Tetrahedron **3**, 339 (1958).

5). N. Shima and H. Aoki, Phys. Rev. Lett. **71**, 4389 (1993).

6). M. Maruyama and S. Okada, Appl. Phys. Express **6**, 095101 (2013)

7). M. Fujita, K. Wakabayashi, K. Nakada, and K. Kusakabe, J. Phys. Soc. Jpn. **65**, 1920 (1996).

8). K. Nakada, M. Fujita, G. Dresselhaus, and M. S. Dresselhaus, Phys. Rev. B **54**, 17954 (1996).

9). Y. Miyamoto, K. Nakada, and M. Fujita, Phys. Rev. B **59**, 9858 (1999).

10). A. Yamanaka and S. Okada, Carbon **96**, 351 (2016).

11). M. Maruyama, N. T. Cuong, and S. Okada, Carbon **109**, 755 (2016).

12). M. Maruyama and S. Okada, Carbon **125**, 530 (2017).

13). O. Ermer, R. Gerdil, and J. D. Dunitz, Helv. Chim. Acta. **54**, 2476 (1971).

14). J. Altman, D. Becker, D. Ginsburg, and H. J. E. Leewenthal, Tetrahedron Lett. **8**, 757 (1967).

15). R. G. D. Taylor, C. G. Bezzu, M. Carta, K. J. Msayib, J. Walker, R. Short, B. M. Kariuki, and N. B. McKeown, Chem. Euro. J. **22**, 2466 (2016).

16). N. V. Krainyukova and E. N. Zubarev, Phys. Rev. Lett. **116**, 055501 (2016).

17). H. Hart, S. Shamouilian, and Y. Takehira, J. Org. Chem. **46**, 4427 (1981).

18). C.-F. Chen, Chem. Commun. **47**, 1674 (2011).

19). T. M. Swager, Acc. Chem. Res. **41**, 1181 (2008).

20). M. Mastalerz and I. M. Oppel, Angew. Chem. Int. Ed. 51, 5252 (2012).

21). P. Kissel, D. J. Murray, W. J. Wulftange, V. J. Catalano, and B. T. King, Nat. Chem. **6**, 774 (2014).

22). T. Kawai, S. Okada, Y. Miyamoto, and A. Oshiyama, Phys. Rev. B **72**, 035428 (2005).

23). D. F. Perepichka, M. Bendikov, H. Meng, and F. Wudl, J. Am. Chem, Soc. **125**, 10190 (2003).

24). J.-S. Yang, J.-L. Yan, C.-Y. Hwang, S.-Y. Chiou, K.-L. Liau, H.-H. G. Tsai, G.-H. Lee, and S.-M. Peng, J. Am. Chem. Soc. **128**, 14109 (2006).

25). M. Xue and C.-F. Chen, Chem. Commun. **47**, 2318 (2011).

26). J. Sorimachi and S. Okada, Phys. Rev. B **96**, 024103 (2017).

27). P. Hohenberg and W. Kohn, Phys. Rev. **136**, B864 (1964).

28). W. Kohn and L. J. Sham, Phys. Rev. **140**, A1133 (1965).

29). Y. Morikawa, K. Iwata, and K. Terakura, Appl. Surf. Sci. **169-170**, 11 (2001).

30). J. P. Perdew, K. Burke, and M. Ernzerhof, Phys. Rev. Lett. **77**, 3865 (1996).

31). D. Vanderbilt, Phys. Rev. B **41**, 7892 (1990).

32). M. Maruyama, N. T. Cuong, and S. Okada, J. Phys. Soc. Jpn. **84**, 084706 (2015)

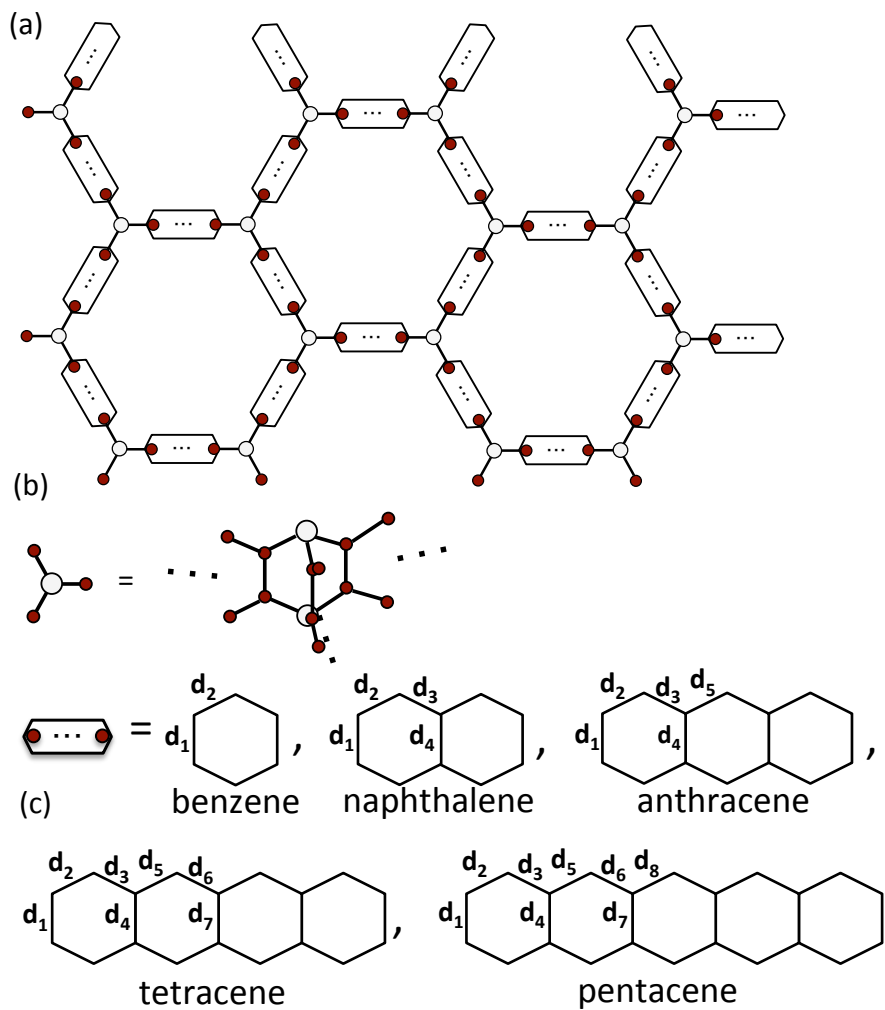33). M. Maruyama and S. Okada, Diam. Relat. Matter. **81**, 103 (2018)

Fig. 1. (Color online) (a) A schematic view of the geometric structures of two-dimensional covalent networks consisting of (b) bridgehead sp^3 C atoms and (c) oligoacenes ranging from benzene to pentacene. Empty and filled circles indicate C atoms with fourfold and threefold coordination, respectively.
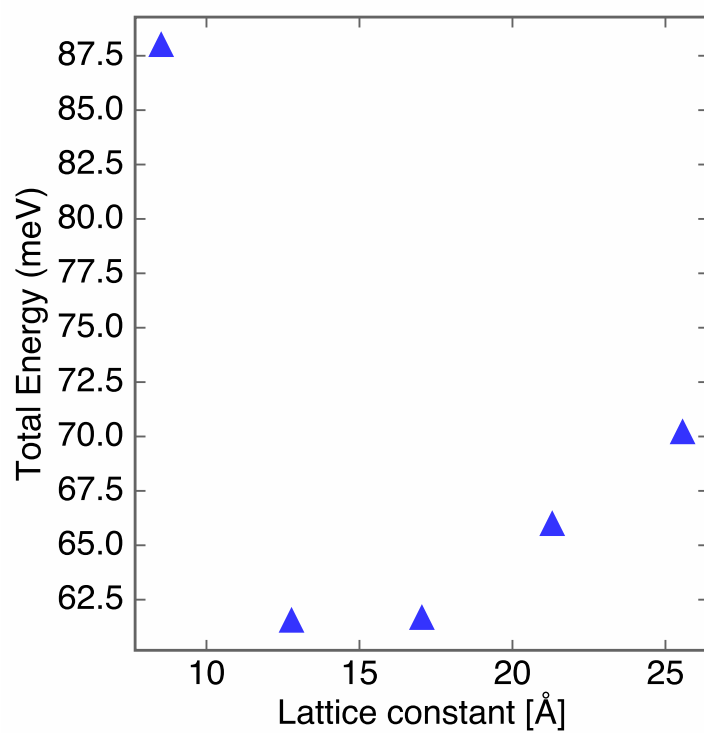
Fig. 2. (Color online) Total energy of the two-dimensional covalent networks consisting of oligoacene and sp^3 C atoms as a function of the lattice constant. The energy is measured from that of an isolated graphene.
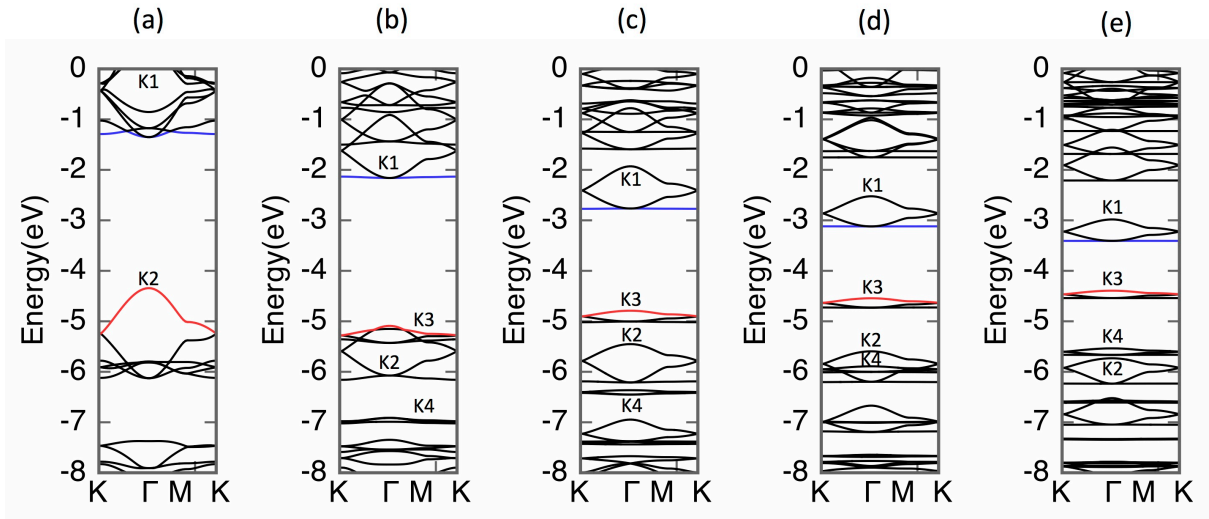
Fig. 3. (Color online) Electronic structures of the two-dimensional covalent networks containing (a) benzene, (b) naphthalene, (c) anthracene, (d) tetracene, and (e) pentacene. Indexes indicate the Kagome bands. The vacuum level energy is set to zero. Red and blue bands indicate the highest occupied and the lowest unoccupied states, respectively.
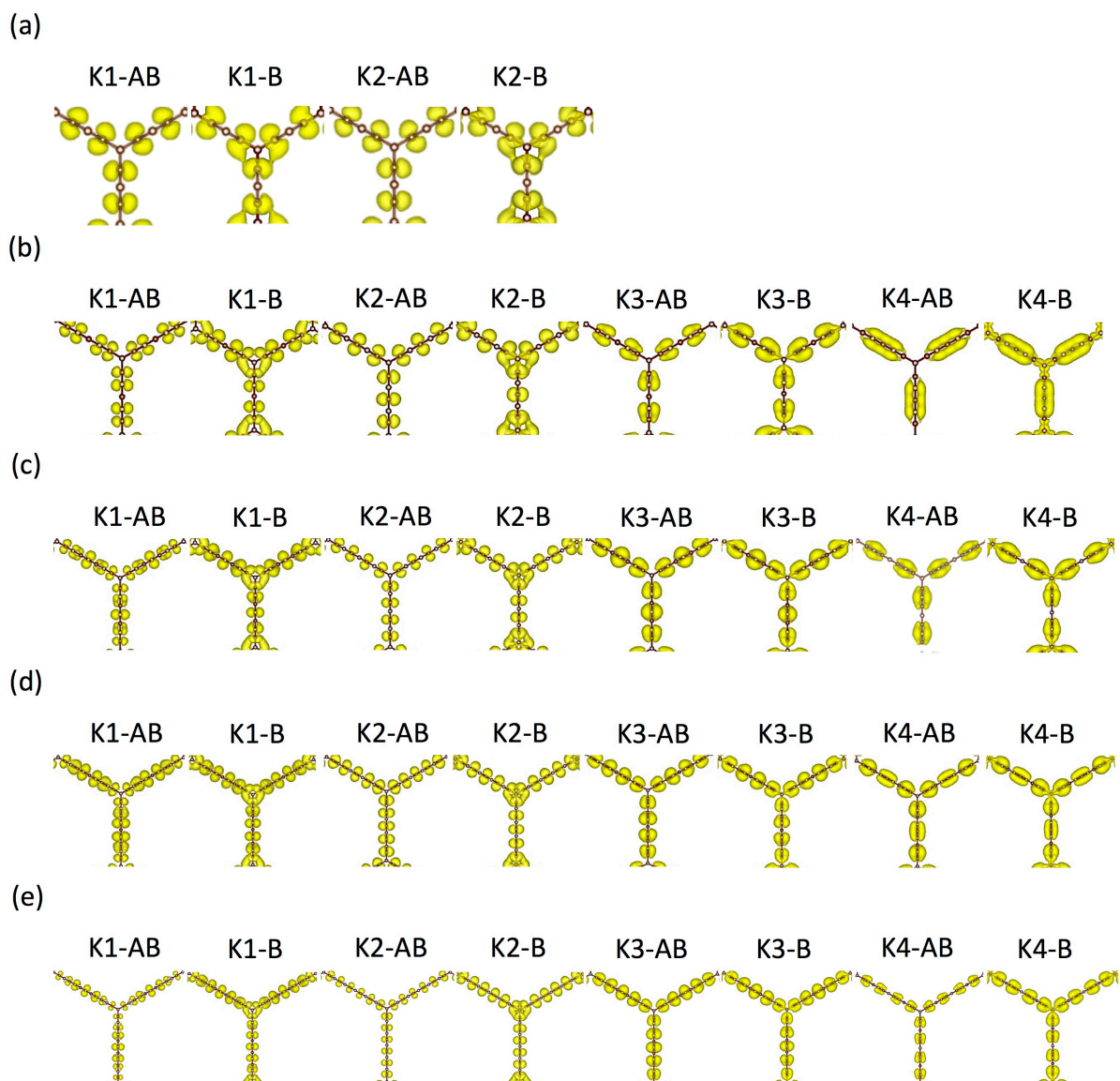
Fig. 4. (Color online) Isosurfaces of the squared wave functions of the Kagome bands at the Γ point of the two-dimensional covalent networks containing (a) benzene, (b) naphthalene, (c) anthracene, (d) tetracene, and (e) pentacene. Indexes correspond to the Kagome band in Fig. 3. Sub-indexes of "–B" and "–AB" indicate the lower and upper branches of each Kagome band.
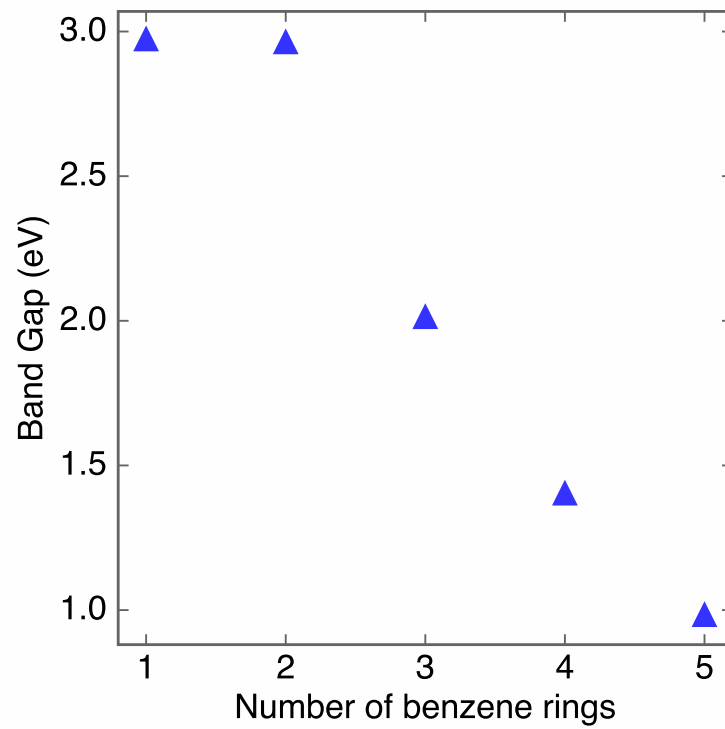
Fig. 5. (Color online) The band gap of the two-dimensional covalent networks consisting of oligoacene and sp^3 C atoms as a function of the number of benzene rings of oligoacene.
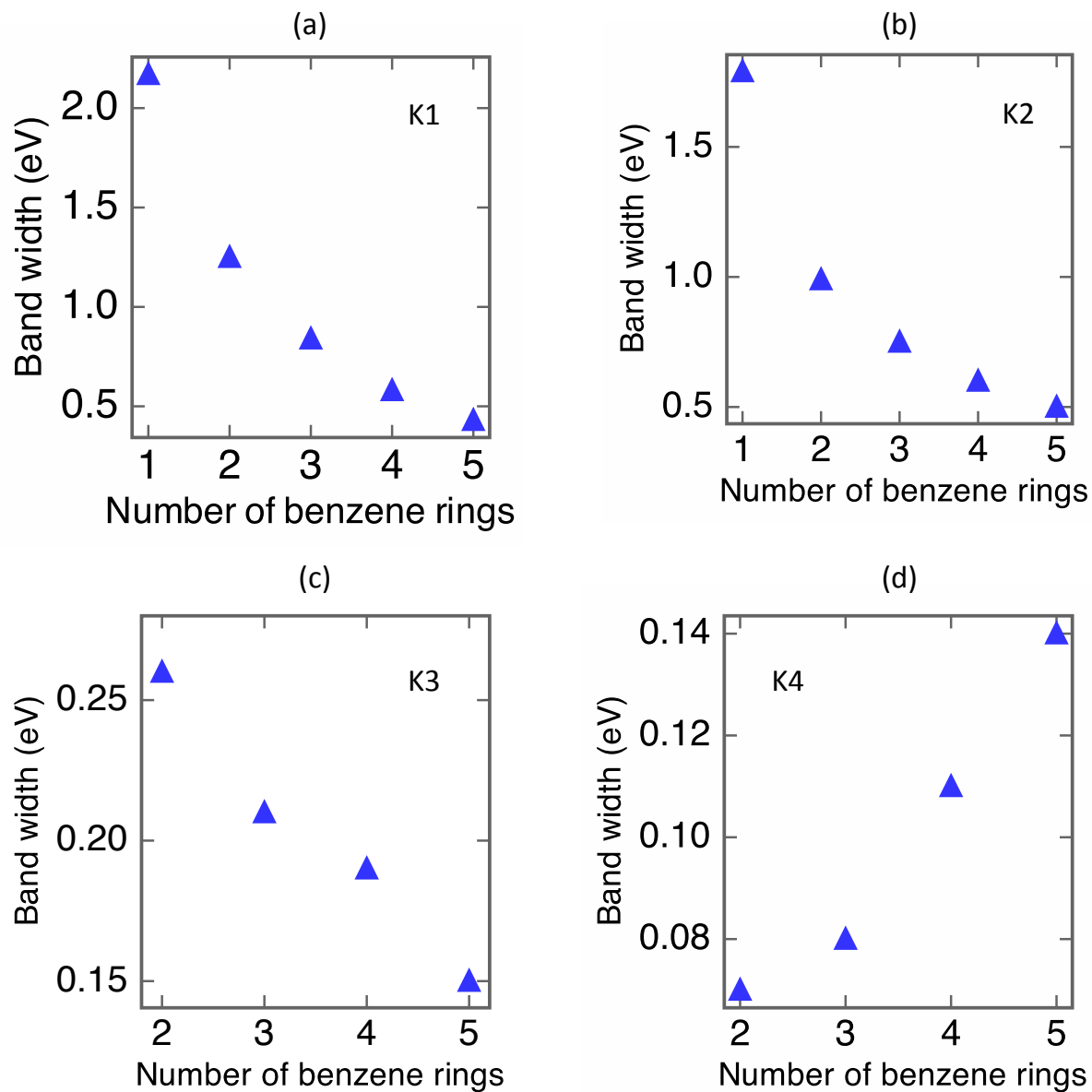
Fig. 6 (Color online) The bandwidth of the Kagome bands (a) K1, (b) K2, (c) K3, and (d) K4 of the two-dimensional covalent networks consisting of oligoacene and sp^3 C atoms as a function of the number of benzene rings of oligoacene.

Table 1. The bond length of the optimized structure of the two-dimensional covalent networks of sp^2 and sp^3 C atoms. The bond labels correspond to the labels in Fig. 1.

oligoacene	Bond length (Å)							
	d1	d2	d3	d4	d5	d6	d7	d8
benzene	1.39	1.38	-	-	-	-	-	-
naphthalene	1.41	1.36	1.41	1.43	-	-	-	-
anthracene	1.42	1.36	1.42	1.44	1.39	-	-	-
tetracene	1.43	1.35	1.42	1.44	1.38	1.40	1.44	-
pentacene	1.43	1.35	1.42	1.45	1.38	1.41	1.45	1.39